Complexing Mechanism of the Lanthanide Cations Eu^{3+}, Gd^{3+}, and Tb^{3+} with 1,4,7,10-Tetrakis(carboxymethyl)-1,4,7,10-tetraazacyclododecane (dota)—Characterization of Three Successive Complexing Phases: Study of the Thermodynamic and Structural Properties of the Complexes by Potentiometry, Luminescence Spectroscopy, and EXAFS

Juliette Moreau,[a] Emmanuel Guillon,[a] Jean-Claude Pierrard,[a] Jean Rimbault,*[a] Marc Port,[b] and Michel Aplincourt[a]

Abstract: Complexation of the lanthanides Eu^{3+}, Gd^{3+}, and Tb^{3+} with 1,4,7,10-tetrakis(carboxymethyl)-1,4,7,10-tetraazacyclododecane (dota) has been studied in solution by using potentiometry, luminescence spectrometry, and EXAFS. Three series of successive complexes were characterized by at least two of these methods: the immediate $[LnH_n(dota)]^{(n-1)+}$** and intermediate $[LnH_n(dota)]^{(n-1)+}$* complexes with $0 \le n \le 2$, and the final $[Ln(dota)]^-$ complexes. The formation constants of the intermediate and final complexes were determined by using potentiometry. From the results, a complexation mechanism involving three steps has been proposed. In the $[LnH_n(dota)]^{(n-1)+}$** complexes that are instantaneously formed, the lanthanide is bound to four oxygen atoms of the carboxylate groups and to five water molecules. These species evolve rapidly: the lanthanide moves into the macrocycle cavity, two new bonds are formed with two nitrogen atoms diametrically opposed in the tetraaza cycle and only three water molecules remain bound to the lanthanide in the $[LnH_n(dota)]^{(n-1)+}$* $(0 \le n \le 2)$ complexes, which appear after a two-day wait. These compounds are stable for about four days. After 4–8 weeks, a concerted rearrangement occurs which leads to the formation of thermodynamically stable $[Ln(dota)]^-$ complexes in which the lanthanide is bound to four nitrogen atoms, four carboxylate oxygen atoms, and one water molecule.

Keywords: EXAFS spectroscopy · lanthanides · luminescence · macrocyclic ligands · potentiometry

Introduction

Medical imagery by nuclear magnetic resonance (NMRI), which is a privileged noninvasive radiological examination technique, has experienced significant developments in recent years. This technique provides anatomic images that correspond to the mapping of protons (^{1}H NMR spectroscopy) in various tissues. Water molecules are responsible for most of the signals. Image contrast, which depends on the density of the protons and their relaxation speed, may be significantly increased by introducing a highly paramagnetic substance. Increased relaxation effectiveness, that is, relaxivity, depends on the dipole interactions between the magnetic moment of a metal ion and the nuclear spin of the protons of the water molecules, on the one hand, and the number of water molecules bound to the metal cation and their exchange speed with the solvent,[1–6] on the other hand.

On account of its high magnetic moment (seven single electrons) and its relatively long electron relaxation time, the Gd^{3+} ion seems to be the most suitable cation for this purpose.[1] The increased relaxation speed of the protons in the water molecules in Gd^{3+} complexes is mainly attributed to three phenomena:[7] the exchange between the water molecule(s) bound to the Gd^{3+} cation in the complex and those of the solvent, denoted as the inside sphere contribution, the diffusion of the water molecules encircling the paramagnetic complex, called the outside sphere contribution, and the exchange of protons in the complex, called the prototropic contribution.

The use of gadolinium as a contrast agent is unfortunately limited by its very high intrinsic toxicity. Its use in vivo assumes that it will be injected into the blood in the form of a

[a] Dr. J. Moreau, Dr. E. Guillon, Dr. J.-C. Pierrard, Prof. J. Rimbault, Prof. M. Aplincourt
GRECI, Université de Reims Champagne-Ardenne
BP1039, 51687 Reims Cedex 2 (France)
Fax: (+33) 0326-913-243
E-mail: jean.rimbault@univ-reims.fr
michel.aplincourt@univ-reims.fr

[b] Dr. M. Port
Centre de Recherche Guerbet, Guerbet, BP50400
95943 Roissy CdG Cedex (France)

DOI: 10.1002/chem.200400006

kinetically and thermodynamically very stable complex to prevent any dissociation before its excretion. Many competing equilibria contribute to the in vivo dissociation of gadolinium complexes: the protonation of the ligand, the complexation of the ligand with Ca^{2+}, Zn^{2+}, and Cu^{2+} ions present in the environment (transmetallation), as well as the precipitation of the Gd^{3+} salts. The charge density, the size of the metal ion and the rigidity of the ligand are the principal factors affecting their stabilities and dissociation speed in the presence of protons. In general, polyaminocarboxylic ligands and, in particular, macrocyclic polyaminocarboxylic ligands are capable of forming complexes with gadolinium(III) ions. 1,4,7,10-Tetrakis(carboxymethyl)-1,4,7,10-tetraazacyclododecane (dota), whose neutral form is written H_4(dota) and whose structure is schematically represented in Scheme 1, forms extremely stable $[Ln(dota)]^-$ complexes in aqueous solution.[1] Their chemical inertia is most likely due to the size of the internal cavity,[8] its conformation,[9] as well as the preorganization[10–12] and rigidity[13–15] of the free ligand. These complexes exist in solution in the form of two pairs of enantiomers of diastereoisomers that are characterized by NMR spectroscopy.[14–17] They present two sources of helicity: the first due to the four five-membered rings formed by the bonds of the acetate arms with the metal ion (absolute configuration Δ or Λ), the second due to the four five-membered rings formed by the bond between the lanthanide and the nitrogen atoms of the macrocycle (absolute configuration $\delta\delta\delta\delta$ or $\lambda\lambda\lambda\lambda$).

Abstract in French: *La complexation des lanthanides Eu^{3+}, Gd^{3+} et Tb^{3+} par le 1,4,7,10-tétrakis(carboxyméthyl)-1,4,7,10-tétraazacyclododécane (dota) est étudiée en solution, par potentiométrie, spectrométrie de luminescence et EXAFS. Trois séries de complexes successifs sont caractérisées par au moins deux de ces méthodes: les complexes instantanés $[LnH_n(dota)]^{(n-1)+}$** et intermédiaires $[LnH_n(dota)]^{(n-1)+}$* avec $0 \le n \le 2$ et les complexes finaux $[Ln(dota)]^-$. Les constantes globales de formation des complexes intermédiaires et finaux sont déterminées par potentiométrie. L'ensemble des résultats permet de proposer un mécanisme de complexation qui comporte trois étapes. Dans les complexes $[LnH_n(dota)]^{(n-1)+}$** formés instantanément, le lanthanide est lié à quatre atomes d'oxygène des groupes carboxylates et à cinq molécules d'eau. Ces composés évoluent rapidement, le lanthanide pénètre dans la cavité du macrocycle en formant deux nouvelles liaisons avec deux atomes d'azote diamétralement opposés du cycle tétraaza et il ne subsiste plus que trois molécules d'eau liées au lanthanide dans les complexes $[LnH_n(dota)]^{(n-1)+}$* ($0 \le n \le 2$) formés après deux jours d'attente. Ces composés sont stables pendant environ 4 jours. Après 4—8 semaines, un réarrangement concerté au sein des complexes conduit à la formation des composés thermodynamiquement stables $[Ln(dota)]^-$ dans lesquels le lanthanide est lié à quatre atomes d'azote, quatre atomes d'oxygène carboxylate et à une molécule d'eau.*

The literature covering the complexation of lanthanides with dota or its derivatives has particularly proliferated in the last 15 years. In the study of Ln^{3+}–dota systems, many of the authors were surprised by the slowness of the formation of the thermodynamically stable complexes.[7,13,18–21] At room temperature, it is necessary to wait 4–6 weeks and even longer for their formation equilibria to stabilize. On account of the slowness of these kinetics, the method of separate solutions[7,22–25] has to be used to determine the formation constants of the thermodynamically stable complexes. The divergence of the results obtained for the Gd^{3+}–dota system was underscored by a number of authors, including Toth[24] and Comblin[26] and their co-workers. There are very few results covering the Eu^{3+}–dota and Tb^{3+}–dota systems and these results are also very divergent.[27–30] The values of the formation constants β_{110} for the $[Ln(dota)]^-$ complexes vary over five logarithmic units (from 23.5 to 28.5).

Prior to the slow formation of the final thermodynamically stable complex, various "protonated" intermediate complexes[2] are rapidly formed during the mixing of a dota solution with a lanthanide salt that are stable for a sufficiently long time to be studied. These intermediate complexes have been identified by various techniques: kinetic measurements[20,22] for Eu^{3+}– and Ce^{3+}–dota, NMR,[21] absorption spectroscopy,[18,24] luminescence,[31] potentiometry[7,23] and some of their structures have been confirmed by molecular modeling.[31]

All of the experimental results published in the literature may be grouped together into two "complexing" mechanisms.

The first complexing mechanism, proposed by Wu and Horrocks,[31] Burai,[32] Brucher,[18] Toth,[24] Jang,[33] Szilagyi,[22] and Chang,[12] and their co-workers, is a three-phase mechanism.

Phase I involves the formation of the $[LnH_2(dota)]^+$ complex in which the Ln^{3+} ion is located outside the cage formed by the four nitrogen atoms and the four oxygen atoms of the carboxylic groups. The two protons bound to two diametrically opposed nitrogen atoms of the tetraaza ring are oriented towards the inside of the cage. The Ln^{3+} ion is only bound to the four oxygen atoms of the carboxylic groups and is located above the plane formed by these four atoms because of the repulsion by the protons of the tetraaza ring. The coordination number of nine for the lanthanide cation is assured by five water molecules.

During Phase II, the $[LnH_2(dota)]^+$* complex loses a proton from a nitrogen atom to form [LnH(dota)]* without changing the bonding modes.

In Phase III, there is a concerted rearrangement of the intermediate complex [LnH(dota)]*: the Ln^{3+} ion slowly penetrates the cage formed by the eight atoms (four nitrogen atoms of the ring and four oxygen atoms of the carboxylic

[1] For all the lanthanide complexes ($Ln^{3+} = Eu^{3+}$, Gd^{3+}, and Tb^{3+}), the coordination number of nine is assured by capped water molecules, which are often omitted for clarity.

[2] The formulae of the intermediate complexes will always be followed by an asterisk to distinguish them from the final thermodynamically stable complexes.

groups) and at the same time the intermediate complex [LnH(dota)]* loses its last proton to form the intermediate complex $[Ln(dota)]^-$ in which the four nitrogen atoms of the ring and the four oxygen atoms of the carboxylic groups are bound to the Ln^{3+} ion. The coordination number of nine for the lanthanide cation is assured by a water molecule.

The release of the protons from the nitrogen atoms of the ring in the intermediate complexes is envisioned to occur by two reaction paths. The first path already suggested by Toth et al.[24] involves the direct insertion of OH^- or H_2O into the coordination cage, while in the second path, Kumar and Tweedle[13] propose a prior inversion of the proton in the tetraaza ring, in which the proton moves from the inside to the outside of the coordination cage. The structural models of the intermediate complexes show that these protons are barely accessible to the solvent. The plausibility of the first path depends on the flexibility of the intermediate complexes. Although the lability of the Y–acetate[24,31] bond in $[YH_2(dota)]^{+}$* allows access to the proton of the nitrogen atom, this is not the case for [YH(dota)]*, which has a rigid structure due to the formation of a new bond between the lanthanide and a nitrogen atom in the ring. This first path is therefore plausible only for Phase I. The second path may be eliminated because the energy barrier to inversion of a quaternary ammonium compound is very high. Jang et al.[33] proposed a third path which is extremely favorable for reaction (1), which involves the transfer of a proton from an NH^+ group in the ring to an oxygen atom of one of the carboxylic groups, which facilitates its accessibility by OH^- or H_2O. Concomitant with this transfer, Y^{3+} moves from the outside to the inside of the coordination cage. Molecular models of $[YH_2(dota)]^{+}$* and [YH(dota)]* show that the position of the proton is extremely favorable for this transfer (distances and angle). The energy barrier to this migration is not very high, which favors this hypothesis. This path is exactly the inverse of the path proposed for the dissociation of $[Y(dota)]^-$ catalyzed by H^+: protonation of a carboxy site and then a transfer of the proton attached to a nitrogen atom in the ring followed by electrostatic repulsion of Y^{3+} and the proton, which favors dissociation.[20,21,24,34]

$$[YH(dota)]^* \rightarrow [Y(dota)]^- + H^+ \quad (1)$$

The second complexing mechanism proposed by Kumar and Tweedle,[13] Wang et al.,[21] Kasprzyk and Wilkins,[20] Bianchi et al.[7,23] involves the following two phases.

Phase I involves the very fast formation of a singly protonated intermediate complex of the formula [LnH(dota)]* [reaction (2)]. In this form, the proton is located on a nitrogen atom in the tetraaza ring, the lanthanide cation is coordinated to the four oxygen atoms of the carboxylic groups and to at least one nitrogen atom in the tetraaza ring and is located in the plane of the four oxygen atoms of the carboxylic groups.

$$Ln^{3+} + H_2(dota)^{2-} \overset{\text{fast}}{\rightleftharpoons} [LnH(dota)]^* + H^+ \quad \text{intermediate complex} \quad (2)$$

In Phase II the intermediate complex [LnH(dota)]* loses its last proton (reaction favored by OH^- or H_2O) [reaction (3)]. A rearrangement takes place in the complex and the Ln^{3+} cation slowly penetrates the coordination cage. The proton of the NH^+ group may transiently migrate to the carboxylate group during this phase.

$$[LnH(dota)]^* \rightarrow [Ln(dota)]^- + H^+ \quad \text{final complex} \quad (3)$$

Table 1. Logarithmic values of the successive protonation constants K_{0lh} of dota.[a]

Electrolyte functional group[b]	Ionic strength	T [°C]	$\log K_{011}$ NH^+	$\log K_{012}$ NH^+	$\log K_{013}$ COOH (2)	$\log K_{014}$ COOH (2)	$\log K_{015}$ COOH (1)	$\log K_{016}$ COOH (1)	pK_w
NaCl[39]	1	37	10.80	9.00	4.24	4.05			
NaCl[40]	0.1	25	9.37	9.14	4.63	3.91			
NaCl[35]	0	25	11.08	9.23	4.24	4.18	1.88	1.71	
KCl[40]	0.1	25	11.14	9.50	4.61	4.30			
KCl[41]	0.1	25	11.36	9.73	4.54	4.41			
KCl[36]	0.1	25	11.14	9.69	4.84	3.95			13.78
KNO_3[42]	0.1	25	11.22	9.75	4.37	4.36			
NMe_4Cl[7]	0.1	25	11.74	9.76	4.68	4.11	2.37		13.83
NMe_4Cl[30]	0.1	25	11.22	9.64	4.86	3.68			13.90
NMe_4Cl[40]	0.1	25	11.73	9.40	4.50	4.19			13.78
NMe_4Cl[43]	0.1	25	12.00	9.70	4.67	4.13	2.38		
NMe_4Cl[32]	0.1	25	12.60	9.70	4.50	4.14	2.32		13.84
NMe_4NO_3[44]	0.1	25	12.12	9.67	4.55	4.14			
NMe_4NO_3[45]	0.1	25	12.09	9.76	4.56	4.09			
NMe_4NO_3[42]	0.1	25	12.09	9.68	4.55	4.13			
NMe_4Cl this work	0.1	25	11.45(2)	9.64(1)	4.60(1)	4.11(1)	2.29(2)		13.78

[a] K_{0lh} refers to the equilibrium $H_{h-1}(dota) + H^+ \rightleftharpoons H_h(dota)$. Values in parentheses represent 1σ standard deviation. [b] Indexing is according to reference [35] and Scheme 1.

The stabilities of the intermediate and final complexes of the Ln^{3+}–dota systems ($Ln^{3+}=Gd^{3+}$, Eu^{3+}, Tb^{3+}) determined in earlier work show poor agreement (see Tables 2 and Table 3). The divergences in the stability of the final complex may be due to either the use of an inappropriate background salt, because the alkaline ions and, in particular, Na^+ are complexed by dota,[30,35,36] or insufficient experimental time to study the formation of the final complex. The addition of an auxiliary ligand,[7,23,37] as used by some authors, also introduces an additional source of error because perfect knowledge of the complexation of the auxiliary ligand under the same experimental conditions as those selected to study the complexation of dota.

In recent work,[38] the joint use of complementary techniques in solution (potentiometry, luminescence spectroscopy, and EXAFS) allowed us to identify the coordination mechanism of a derivative of dota (the tetracarboxyethyl dota or tce-dota) with three lanthanide cations (Eu^{3+}, Gd^{3+}, and Tb^{3+}). Potentiometry allows the number and stoichiometry of the various complexes present in solution to be derived, the determination of their relative stabilities and the position of the protons in the complexes to be specified by calculating their acidity constants. The study of the Ln^{3+} environment by EXAFS allows the number, the nature and the length of the bonds formed between the lanthanide cation and the ligand or the solvent to be determined. Luminescence spectroscopy allows the number of water molecules bound to europium or terbium to be confirmed by lifetime measurements. It seemed worthwhile to use these techniques to study the complexation of dota in solution to explain the apparently contradictory results reported in the literature.

Table 2. Logarithmic values of the overall formation constants and the corresponding successive protonation constants for the $[LnH_n(dota)]^{(n-1)+*}$ complexes.[a]

Authors	Experimental conditions	Eu^{3+}	Gd^{3+}	Tb^{3+}
Wu and Horrocks[31]	KCl (0.1 mol L^{-1}), 25 °C	$\log\beta_{112}^*=26.71$		
		$\log\beta_{111}^*=23.18$		
		$\log K_1^*=3.53$		
Burai et al.[32]	KCl (0.1 mol L^{-1}), 25 °C			$\log\beta_{111}^*=26.5$[b]
Toth et al.[24]	NaCl (1 mol L^{-1}), 25 °C	$\log\beta_{112}^*=25.30$		$\log\beta_{112}^*=25.30$[b]
Wang et al.[21]	NaCl (1 mol L^{-1}), 25 °C		$\log\beta_{111}^*=22.10$	
Bianchi et al.[7,23]	NMe_4Cl (0.1 mol L^{-1}), 25 °C		$\log\beta_{111}^*=24.5(1)$	
			$\log\beta_{110}^*=21.2(1)$	
			$\log K_2^*=3.3(1)$	
this work	NMe_4Cl (0.1 mol L^{-1}), 25 °C	$\log\beta_{112}^*=29.35(7)$	$\log\beta_{112}^*=30.41(10)$	$\log\beta_{112}^*=30.05(12)$
		$\log\beta_{111}^*=26.64(4)$	$\log\beta_{111}^*=27.67(8)$	$\log\beta_{111}^*=27.35(9)$
		$\log\beta_{110}^*=24.02(5)$	$\log\beta_{110}^*=24.99(9)$	$\log\beta_{110}^*=24.91(10)$
		$\log K_1^*=2.71(4)$	$\log K_1^*=2.75(2)$	$\log K_1^*=2.70(4)$
		$\log K_2^*=2.62(2)$	$\log K_2^*=2.68(1)$	$\log K_2^*=2.44(2)$

[a] NMe_4Cl 0.1 mol L^{-1}, 25 ± 0.1 °C. $\log K_n^*$ refers to the equilibrium $[LnH_{n-1}(dota)]^{(n-2)+*}+H^+\rightleftharpoons[LnH_n(dota)]^{(n-1)+*}$. Values in parentheses represent 1σ standard deviation. [b] Ce^{3+} complexes.

Table 3. Logarithmic values of the overall formation constants β_{110} of the thermodynamically stable species $[Ln(dota)]^-$ (Ln = Gd, Eu, Tb).[a]

References	Background salt	Ionic force	T [°C]	Ln^{3+}	$\log\beta_{110}$
[7]	NMe_4Cl	0.1	25	Gd^{3+}	24.67
[28]	NMe_4Cl	0.1	25		24.70
[25]	NMe_4Cl	0.1	25		24.00
[47]	NMe_4Cl	0.1	25		25.40
[44]	NMe_4NO_3	0.1	25		27.00
[40]	NaCl	0.1	25		25.30
[48]	NaCl	0.1	25		25.10
[27]	KCl	0.1	25		26.03
this work	NMe_4Cl	0.1	25		25.58(5)
[30]	KCl	0.1	25	Eu^{3+}	26.21
[27]	NaCl	0.1	–		23.4
this work	NMe_4Cl	0.1	25		26.48(8)
[27]	NaCl	0.1	–	Tb^{3+}	24.2
this work	NMe_4Cl	0.1	25		26.97(9)

[a] Values in parentheses represent 1σ standard deviation.

Results and Discussion

Potentiometric study: This study was carried out under argon at 25 °C in an NMe_4Cl (0.1 mol L^{-1}) medium. The use of this background salt is more appropriate than that of an alkaline salt because alkaline cations are complexed by dota.[30,35,36]

Protonation of dota: dota, whose neutral form is written H_4(dota), has four ionizable protons and eight potential protonation sites, the four nitrogen atoms and the four carboxylate groups (Scheme 1).

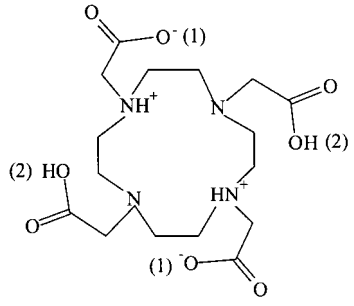

Scheme 1. Protonation sites of dota.

The successive protonation constants of dota, as well as their assignments to the various protonation sites, are listed in Table 1. The assignments were accomplished without ambiguity by an ^{1}H NMR study of the CH_2 groups of the molecule.[35] The value of the ionic product of water determined under various experimental conditions is indicated in the last column of Table 1. This value must be determined with the highest precision because it has a big influence on the value of the first protonation constant K_{011} of dota; a variation in the pK_w of ± 0.02 units induces a variation of approximately ± 0.3 units in $\log K_{011}$.

Complexation of the lanthanides in solution: The complexation kinetics of the Ln^{3+}–dota systems were followed by potentiometry at 20 °C. The pH of a dota solution is markedly reduced by approximately 0.8 units as soon as the metal salt is added (Figure 1), and then continues to decrease slowly and regularly for two days. The pH is then stabilized for 3–4 days (formation of the intermediate complexes) and then again decreases slowly until it is definitively stabilized after 6–7 weeks (formation of the final thermodynamically stable complex).

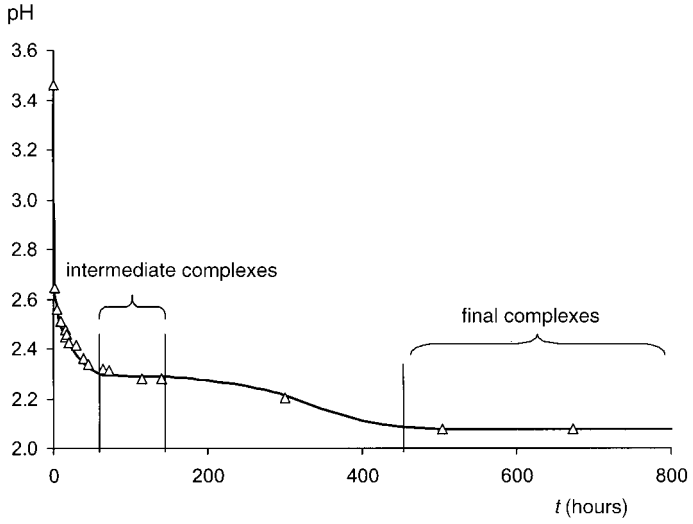

Figure 1. pH variation of an equimolar solution of Eu^{3+} and dota versus time. $[Eu^{3+}] = [dota] = 2.4 \times 10^{-3}$ mol L^{-1}.

An increase in temperature accelerates the rate of formation of the final complex. Thus at 50 °C the pH of a solution identical to the previous one is stable for seven weeks after a wait time of only one week, but it varies again slightly after 10 weeks, which may be due to a slight degradation of the ligand at this temperature. The addition of the auxiliary ligand edta proposed by some authors does not accelerate the kinetics. It does not reverse the complexation equilibrium and, as a result, addition of a strong acid will be preferred.

[3] The formulae of these barely stable, instantaneously formed, complexes will always be followed by two asterisks to distinguish them from the stable intermediate complexes $[LnH_n(dota)]^{(n-1)+}$* and the final thermodynamically stable complexes $[Ln(dota)]^-$.

The marked variation in pH as soon as the lanthanide salt and dota were mixed corresponds to the instantaneous formation of the $[LnH_2(dota)]^{+}$** complexes.[3] It was not possible to determine the formation constants of the immediate complexes. Extrapolation to time zero of the increasing and linear section of the curves representing $\log\beta_{mlh}$ (β_{mlh} refers to the species $M_mL_lH_h$) versus the stabilization time of the initial mixture (see Figure 3) would lead to erroneous values of $\log\beta_{mlh}$ because the formation kinetics are very fast and consequently the complexes evolve for the time required to assure the titration of the solutions (four points were measured in an hour).

Their formulae, as well as the coordination mode of the lanthanide ions in these compounds, were determined during the study of the solutions by EXAFS and by luminescence in the case of europium or terbium (vide infra). The formation of the intermediate complexes $[LnH_n(dota)]^{(n-1)+}$* and the final complexes $[Ln(dota)]^-$ were studied by potentiometry.

*Formation of the intermediate complexes $[LnH_n(dota)]^{(n-1)+}$**: The experimental titration curve of an equimolar solution of Gd^{3+} and dota titrated against NMe_4OH ($2.2 < pH < 3.5$) is represented in Figure 2, as are the two titration curves calcu-

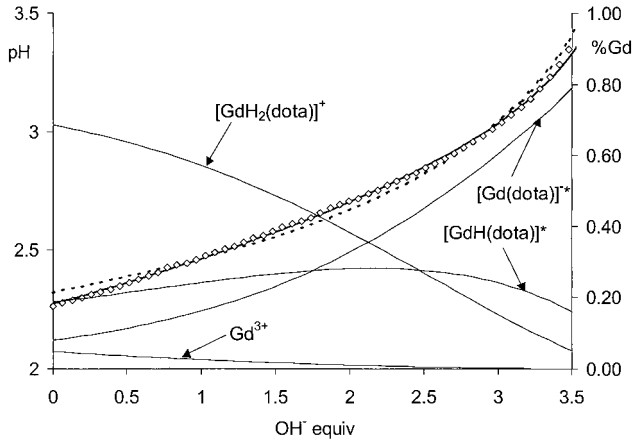

Figure 2. Gd^{3+}–dota system: the initial wait time of the mixture is 73 h. Titration curves of an equimolar solution of gadolinium and dota titrated with NMe_4OH. (◇) experimental points; (-----) titration curve calculated by assuming the presence of [GdH(dota)]* and $[Gd(dota)]^-$*;(——) titration curve calculated by assuming the presence of $[GdH_2(dota)]^+$*, [GdH(dota)]* and $[Gd(dota)]^-$*. Distribution curves (——) of gadolinium between the species Gd^{3+}, $[GdH_2(dota)]^+$*, [GdH(dota)]*, and $[Gd(dota)]^-$*.

lated from the refined values of the formation constants. The wait time for the initial mixture is 73 h. Note that insertion of the $[GdH_2(dota)]^+$* complex into the solution at equilibrium improves the agreement between the experimental points and the titration curve calculated for the pH range studied. The standard deviation on all the points used during the calculations is divided by three; this observation is valid for the three cations studied. The $[GdH_2(dota)]^+$* complex is present in a solution pH 2.2–3.5 as the distribution curves for gadolinium in Figure 2 show. Since the last

points of the strength curve are located above three added base equivalents, it is indispensable to add to the complexes in equilibrium the $[Gd(dota)]^{-}$* complex, whose formation is accompanied by the release of four protons as Bianchi et al.[7] proposed.

Figure 3 shows the logarithmic variation of the formation constants $\log\beta_{mlh}$* of the intermediate complexes of the Gd–dota, Eu–dota and Tb–dota systems versus the wait time of the initial mixture.

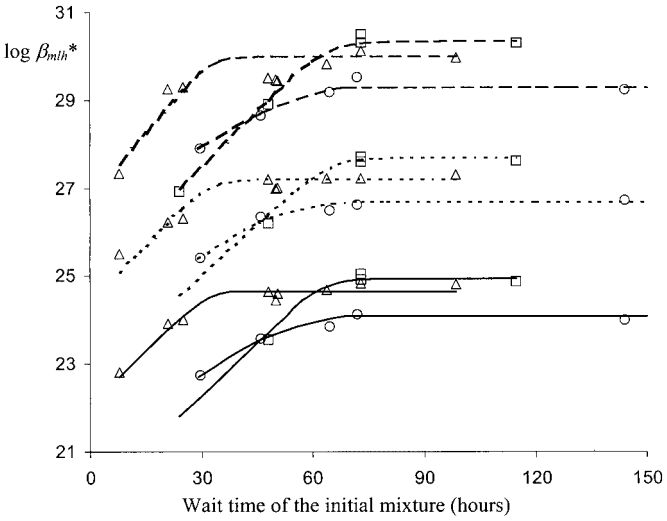

Figure 3. Ln^{3+}–dota systems: logarithmic variation of the formation constants of the intermediate complexes $[LnH_2(dota)]^{+}$*, [LnH(dota)]*, and $[Ln(dota)]^{-}$* versus the wait time of the initial mixture (1–147 h). The stabilization time after each base addition was 15 minutes. (○) Eu^{3+}, (△) Tb^{3+}, (□) Gd^{3+}; (——) $\log\beta_{110}$*; (-----) $\log\beta_{111}$*; (– – –) $\log\beta_{112}$*.

For each lanthanide, an almost linear increase is observed followed by a stabilization of the values of $\log\beta_{mlh}$*. This variation corresponds to the evolution of the complexation kinetics during the wait time of the initial mixture. If the complexation kinetics are not stable before the start of the titration, the contents of the mixture continue to evolve during the titration, which renders the section of the curve that is increasing in $\log\beta_{mlh}$* unexploitable. Under our experimental conditions, the intermediate complexes are formed in 60 h and then are stable for approximately 80 h. Above 150 h, the $[LnH_2(dota)]^{+}$* complex disappears during the evolution of the intermediate complexes to the final complexes $[Ln(dota)]^{-}$.

For each system studied, the use of 3–6 solutions (200–350 points), whose pH values are between 2.2 and 3.5 and which have a variable wait time of between 60 and 140 h, allows the logarithms of the global formation constants of the three intermediate complexes in equilibrium to be calculated. Our results, as well as the bibliographic data, are given in Table 2.

The stabilities of the intermediate lanthanide complexes decrease in the order $Gd^{3+} > Tb^{3+} > Eu^{3+}$. The formation constants for the $[LnH_n(dota)]^{(n-1)+}$* complexes determined in this work are all greater than those calculated by others who used much shorter stabilization times (25–50 min,[7,23] 1–70 min,[24], 45 s–1 h 39 min[31] or immediately after mixing[21]). All this is in agreement with the curves in Figure 3, which indicate that $\log\beta_{mlh}$* increases when the wait time of the initial mixture is insufficient. The values $\log\beta_{112}$* = 26.71 and $\log\beta_{111}$* = 23.18 found by Wu and Horrocks[31] are relatively close to the approximate values obtained from the graph in Figure 3 by extrapolating to zero wait time ($\log\beta_{112}$* ~ 26.4 and $\log\beta_{111}$* ~ 23.8).

Formation of the thermodynamically stable complexes $[Ln(dota)]^{-}$: On account of the high stability of the $[Ln(dota)]^{-}$ complexes, some authors added edta as an auxiliary ligand.[7,23,37] The release of protons from edta and its complexation with gadolinium were therefore studied under conditions identical to those used in the dota study. The logarithms of the global formation constants of the protonated complexes of the ligand and the 1:1 Gd^{3+}–edta complex are respectively $\log\beta_{011} = 10.24(1)$, $\log\beta_{012} = 16.35(2)$, $\log\beta_{013} = 19.20(2)$, $\log\beta_{014} = 20.51(18)$ and $\log\beta_{110} = 17.57(5)$. This last value is close to those reported in the literature [17.7[40] and 17.35[46] in a NMe_4NO_3 (0.1 mol L^{-1}) medium].

The Gd^{3+}–dota system was studied in the presence and absence of edta for two Gd^{3+} concentrations and by stabilizing the solutions for either one week at 50 °C or seven weeks at 20 °C. The consistency of the results is substantiated (Figure 4) by the superposition of the three titration

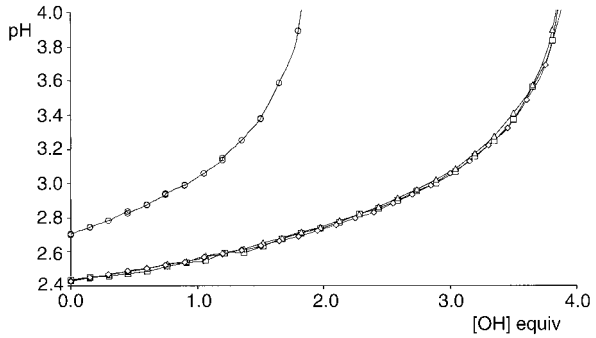

Figure 4. Gd^{3+}–dota system: titration curves of equimolar solutions of Gd^{3+} and ligand titrated with NMe_4OH (0.2 mol L^{-1}) by the "out-of-cell" method: (△) $[Gd^{3+}] = [dota] = 1.0\times10^{-3}$ mol L^{-1}, $T = 50$ °C, wait time of 1 week; (□) $[Gd^{3+}] = 1.0\times10^{-3}$ mol L^{-1}, $[dota] = [edta] = 5.0\times10^{-4}$ mol L^{-1}, $T = 50$ °C, wait time of 1 week; (◇) $[Gd^{3+}] = 1.0\times10^{-3}$ mol L^{-1}, $[dota] = [edta] = 5.0\times10^{-4}$ mol L^{-1}, $T = 20$ °C, wait time of 7 weeks; (○) $[Gd^{3+}] = [dota] = 5.0\times10^{-4}$ mol L^{-1}, $T = 20$ °C, wait time of 7 weeks.

curves of the solutions with the same concentrations of metal and total ligand ($[Gd^{3+}] = [ligand]_{total} = 1.0\times10^{-3}$ mol L^{-1} ; "out-of-cell" method; $T = 20$ or 50 °C; with and without edta) and by obtaining similar $\log\beta_{110}$ values for each of the four series of points. During the study of both of these systems, the solutions were stabilized at 40 °C with wait times of 3–9 weeks.

The $\log\beta_{110}$ values were calculated with the PROTAF program by using each of the series of points ($2.4 < pH < 3.5$) to confirm that the results are in agreement and then with all the points of the four series. Table 3 lists all of our results, as well as the formation constants for the thermodynamically

stable $[Ln(dota)]^-$ complexes found in the literature (Ln^{3+} = Gd^{3+}, Eu^{3+}, and Tb^{3+}; ionic strength = 0.1). The stability of the $[Gd(dota)]^-$ complex ($\log\beta_{110} = 25.40$) determined by Tweedle et al.[47] under experimental conditions identical to ours is relatively close to our result ($\log\beta_{110} = 25.58$).

The stabilities of the final lanthanide complexes decrease in the order $Tb^{3+} > Eu^{3+} > Gd^{3+}$, which differs from that observed during the study of the intermediate complexes ($Gd^{3+} > Tb^{3+} > Eu^{3+}$). All this indicates a difference in the coordination mode of the lanthanide in the intermediate complexes and in the final complexes, which has subsequently been confirmed by EXAFS and luminescence. The terbium complexes are three times more stable than those of europium and 30 times more stable than those of gadolinium. The order of the stabilities is identical to that of the wait times required for the formation of the thermodynamically stable complexes. The rigidity of the coordination cage[13–15] formed by the four nitrogen atoms of the tetraaza ring and the four oxygen atoms of the carboxylate groups seems therefore to be the preponderant factor that determines the high stability of the final complexes.

Luminescence studies: The spectral properties of the ions or complexes of the trivalent lanthanides are closely governed by their electronic structure. The outer lying filled subshells $^5s_2$ $^5p_6$ shield the partially filled ^4f orbitals which are little perturbed by the environment of the metal. Since there is no difference in the parity of the ground state, and the excited state, the electronic transitions are "Laporte forbidden". Consequently, they are characterized by very narrow half-bandwidths in both emission and absorption, very low molar absorptivity and excited-state lifetimes in the order of 1 ms. Some of the Ln^{III} can be distinguished from the metallic cations of the first transition series by their ability to luminesce in solution at room temperature.

Previous work has shown that the decay constant k of these transitions (reciprocal of the lifetime of the excited state), independent of the concentration of the lanthanide ion Eu^{3+} or Tb^{3+}, varies linearly versus the fraction of H_2O in H_2O/D_2O solutions. Numerous empirical relations have been established between the number q of water molecules bound to the metal ion and the difference in the decay constants determined in H_2O and D_2O solutions. In a recent paper, Supkowski and Horrocks[49] also considered the effect of oscillators other than OH. The simplest form of the corrected relation accounts for the effect of water molecules in the outer sphere [Eq. (4)].

$$q = A(k_{H_2O} - k_{D_2O} - 0.31) \quad (4)$$

In a more pragmatic approach, we have considered the decay constants determined for the aqua ions of Eu^{3+} and Tb^{3+} in H_2O/D_2O mixtures by integrating the dynamic quenching of light water molecules in the first and outer spheres. Equation (5) is similar to the first one established by Horrocks and Sudnick,[50], where $A^* = 1.05 \pm 0.02$ for Eu^{III} and $A^* = 4.86 \pm 0.12$ for Tb^{III}. For each complex or aqua ion, Eu^{3+} or Tb^{3+}, the plot of the decay constant k versus the concentration of H_2O in a H_2O/D_2O mixture is a straight line as shown in the graphical representation of the quenching properties of the hydroxy oscillators obtained from the classical Stern–Volmer equation (Figure 5).

$$q = A^*(k_{H_2O} - k_{D_2O}) \quad (5)$$

This involves a statistical equilibrium between successive species of various isotopic compositions and a linear variation of the corresponding decay constants as a function of the number of bound light water molecules.

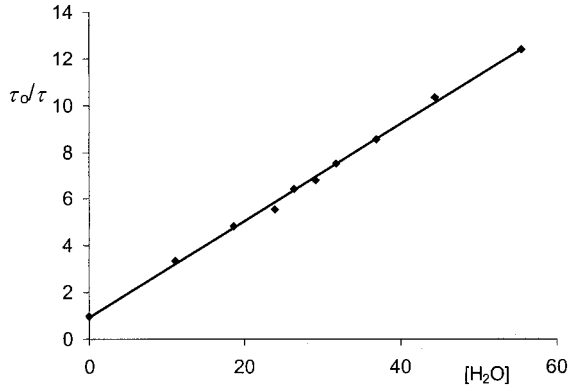

Figure 5. Stern–Volmer plot: water quenching of the initial complexes $[EuH_n(dota)(H_2O)_5]^{(n-1)}$**.

Obviously, there is a correlation between the Stern–Volmer equation and the empirical relation formulated by Horrocks for the europium and terbium complexes [Eq. (6) and Eq. (7)].

$$\tau_0/\tau = 1 + k_q\tau_0[H_2O] \quad (6)$$

$$q = A(k_{H_2O} - k_{D_2O} - \alpha) \quad (7)$$

In the Stern–Volmer relation, τ_0 and τ are the lifetimes of the complexes in the absence and presence of a quencher; the product of the bimolecular quenching constant k_q and the lifetime of the fluorophore τ_o equates to the Stern–Volmer quenching constant K_D.

The number of coordinated water molecules is calculated by using Equation (8), where q is a linear function of k_q, the rate constant for dynamic bimolecular quenching, A is a parameter dependant on the nature of the metal ion and measured in ms, $W = [H_2O]$ (molarity of pure water; $W = 55.509\,mol\,L^{-1}$), and according to Supkowski and Horrocks,[49] α is the contribution of the second coordination sphere water molecules to the quenching of the excited state.

$$q = A(Wk_q \times 10^{-3} - \alpha) \quad (8)$$

From the selected decay data taken from the literature by Supkowski and Horrocks,[49] the corresponding bimolecular quenching constants were determined and plotted against the corresponding q values. The linear least-square fit leads to Equation (9) for the europium complexes.

$$q = 0.0618k_q - 0.3507 \ (r^2 = 0.998) \quad (9)$$

Luminescence data for the terbium complexes are scarce, so only the bimolecular quenching constant determined for the aqua ion $[Tb(H_2O)_8]^{3+}$ is used as a reference parameter and the eventual vibronic quenching contribution of the outer sphere, $q = 0.269.k_q$, is not taken into account.

Three types of complexes are considered. Initial complexes formed immediately after mixing the metal and racemic ligand solutions. The luminescence measurements must be taken immediately after mixing. Intermediate metastable complexes formed after a wait time of 50–100 h. Final complexes obtained and studied after several weeks. The luminescence decay curves were fitted to a decreasing exponential equation with high correlation coefficients except in the case of the experimental data for the intermediate metastable species.

To determine the number of water molecules bound to the europium ion in the metastable species, an equimolar solution of dota and $EuCl_3$ (5×10^{-2} mol L^{-1}) was prepared in H_2O 50 h before the measurements were taken. This solution was then diluted to 1/10 in H_2O and D_2O. The formation constants for the intermediate complexes formation constants derived in the potentiometric study allowed us to determine precisely the composition of the solutions at this time: 23% $[Eu(H_2O)_9]^{3+}$, 5% $[Eu(dota)(H_2O)_q]^{-}$*, 14% $[EuH(dota)(H_2O)_q]$* and 58% $[EuH_2(dota)(H_2O)_q]^{+}$* at pH ~2.1. With the contribution of the nonahydrated europium ion being significant, the experimental data were fitted by using the biexponential Equation (10) with high correlation species.

$$F = F_1^o\exp(-k_1t) + F_2^o\exp(-k_2t) \quad (10)$$

The Stern–Volmer relation τ_0/τ versus the concentration of water is drawn in Figure 6 for the two fluorophores $[Eu(H_2O)_9]^{3+}$ and $[EuH_n(dota)(H_2O)_q]^{(n-1)}$*. In the case of the nonahydrated europium ion the linear relation is verified for all water concentrations and leads to $q = 8.81$. The curve corresponding to the fluorophore $[EuH_n(dota)(H_2O)_q]^{(n-1)}$* ($n = 0, 1, 2$) is a straight line for a concentration of water below 20 mol L^{-1} and leads to $q = 2.79$. The various luminescence parameters determined for all the studied complexes are presented in Table 4.

The number of water molecules bound to the lanthanide ion calculated by using the two relations is very similar. The bimolecular quenching constants k_q, which reflect the accessibility of the water molecules to the lanthanide, are nearly proportional to q. These results are consistent with the fast formation of the initial complexes in which the metal ion is bound to four carboxylate groups and five molecules of water. After waiting for 50 h, the nonahydrated europium ion is in equilibrium with the metastable intermediate complexes. In these species, the metal ion is bound to the four carboxylate groups, three water molecules and two atoms of nitrogen. The final slow kinetic step leads to the formation of the stable monohydrated complexes.

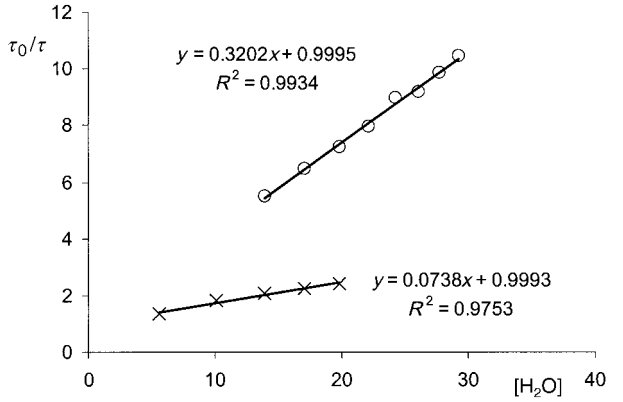

Figure 6. Stern–Volmer plot: water quenching of $[Eu(H_2O)_9]^{3+}$ and $[EuH_n(dota)(H_2O)_q]^{(n-1)}$* in equilibrium. (○) $[Eu(H_2O)_9]^{3+}$; (×) $[EuH_n(dota)(H_2O)_q]^{(n-1)}$*.

EXAFS measurements: X-ray absorption spectroscopy (XAS) experiments were performed to obtain structural information about Ln^{III}–dota complexes, and in particular to gain more detailed information about the intermediate species formed in the reaction between lanthanides and dota. By using the crystal structure of $[Gd(dota)(H_2O)]^{-}$, $[Eu(dota)(H_2O)]^{-}$, and $[Tb(teta)(H_2O)]^{-}$ we calculated their FEFF EXAFS signals. It appears that up to 3.5 Å, multiple scattering may be neglected. Hence, the simulations for all the samples were carried out using the single-scattering model.

First, we studied the initial complexes, that is, after a reaction time between the metallic cation and dota of 1 h. The k^3-weighted experimental and least-squares fitted EXAFS spectra of the $[LnH_2(dota)]^{+}$** intermediate compounds and the corresponding non-phase-shift-corrected Fourier transforms are shown in Figure 7a and 7b, respectively. The results of the least-squares fittings are given in Table 5.

The spectra of Eu^{3+}, Gd^{3+}, and Tb^{3+} are very similar, which indicates that the local structures of the metallic cations are almost the same for all the compounds. Therefore, each intermediate compound has the same number of nearest neighbors. The Fourier transform spectra are composed

Table 4. Luminescence parameters for the europium and terbium species.

Complexes	k_{D_2O} [ms^{-1}]	k_{H_2O} [ms^{-1}]	K_D [L mol^{-1}]	k_q [L mol^{-1}s^{-1}]	q_1[a]	q_2[b]
$[Eu(H_2O)_9]^{3+}$	0.456	8.913	0.3311	150.9	8.98	8.88
$[EuH_n(dota)(H_2O)_5]^{(n-1)}$**	0.400	4.968	0.2067	82.7	4.76	4.79
$[EuH_n(dota)(H_2O)_3]^{(n-1)}$*	0.688	3.507	0.0738	50.8	2.79	2.96
$[Eu(dota)(H_2O)]^{-}$	0.419	1.556	0.0489	20.5	0.92	1.19
$[Tb(H_2O)_8]^{3+}$	0.880	2.525	0.0337	29.7	8.00	7.99
$[TbH_n(dota)(H_2O)_5]^{(n-1)}$**	0.281	1.361	0.0681	19.1	5.15	5.25
$[Tb(dota)(H_2O)]^{-}$	0.272	0.505	0.0145	3.94	1.06	1.13

[a] q_1 was calculated using the relation derived from the Stern–Volmer equation: $q_1 = 0.0618.k_q - 0.3507$ for Eu^{III}; $q_1 = 0.269k_q$ for Tb^{III}. [b] q_2 was calculated by using the Horrocks relation $q_2 = A^*(k_{H_2O} - k_{D_2O})$, with $A^* = 1.05 \pm 0.02$ for Eu^{III} and $A^* = 4.86 \pm 0.12$ for Tb^{III}.

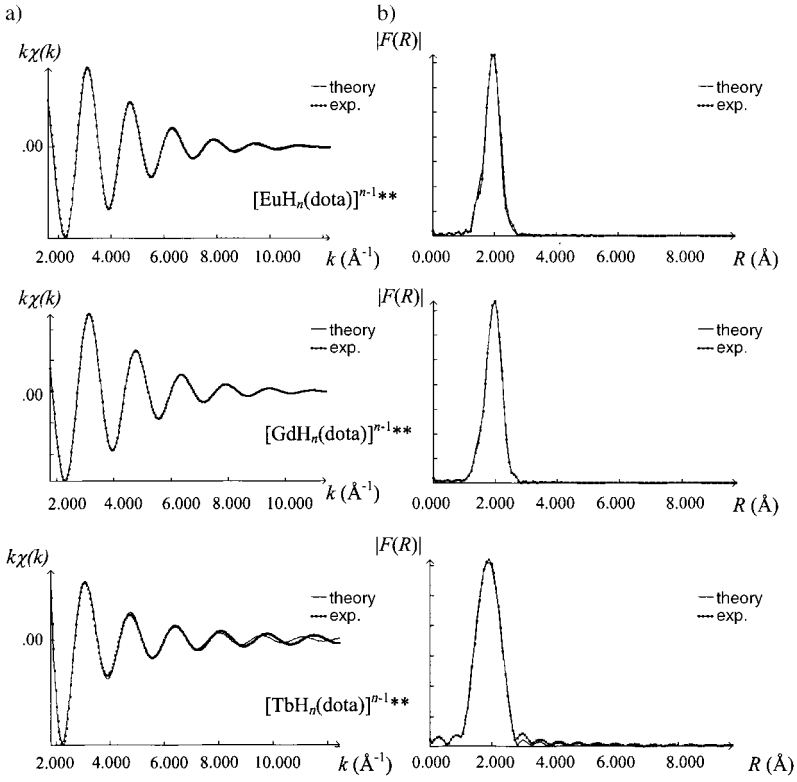

Figure 7. a) k^3-weighted experimental and least-squares fitted first coordination shell EXAFS spectra of the $[LnH_n(dota)]^{(n-1)+}$** intermediate compounds and b) the corresponding non-phase-shift-corrected Fourier transforms.

of one main peak, which corresponds to Ln–O contributions. Within the framework of the single-scattering approach, the $[LnH_2(dota)]^+$** compounds are reasonably fitted if one assumes that Ln^{3+} ions are surrounded by four carboxylate oxygen atoms at an average distance R(Ln–O) of 2.42, 2.39, and 2.37 Å for Eu^{3+}, Gd^{3+}, and Tb^{3+}, respectively. The coordination sphere is completed by five water oxygen (O_w) atoms at a distance R(Ln–O_w) of 2.44 Å for Gd^{3+}, and 2.45 Å for Eu^{3+} and Tb^{3+}. These results are similar to those obtained with the tetracarboxylated derivative of the dota gadolinium complex.[38] Chang et al.[12] previously characterized the Eu^{3+} intermediate ($[EuH_2(dota)]^{+**}$) by molecular modeling with different bond lengths (Eu–O_{COOH} = 2.34 Å, Eu–O_w = 2.60 Å).

In the case of the Gd^{3+} ion, a second intermediate species, $[GdH_2(dota)]^{+*}$, was identified after a wait time of 100 h. Indeed, Figure 8b,II shows the appearance of a new nitrogen contribution at 2.65 Å, and a decrease in the Gd–O contributions relative to the initial complex. By reference to the known final compound $[Gd(dota)]^-$ (Figure 8b,III), we can attribute this contribution to nitrogen atoms in the macrocyclic cavity. The fitting of the EXAFS signals gives the following results (Table 5): the gadolinium ion is still strongly bonded to the four carboxylic oxygen atoms (Gd–O_{COOH} = 2.40 Å), and the first coordination sphere is completed by two macrocyclic nitrogen atoms at a distance close to 2.65 Å, and only three water molecules at 2.41 Å. Several authors have proposed, on the basis of molecular modeling and protometric studies, the existence of the intermediate $[GdH_2(dota)]^{+*}$ species, but, to our knowledge, this study is the first which gives some structural information about the environment of the gadolinium ion.

Finally, after several weeks, the final complexes were obtained and studied by EXAFS. The k^3-weighted experimental and least-squares fitted EXAFS spectra of the $[Ln(dota)]^-$ final compounds, and the corresponding non-phase-shift corrected Fourier transforms are shown in Figure 9a and 9b, respectively.

Moreover, for the gadolinium compound, the evolution of the EXAFS spectrum and the corresponding Fourier trans-

Table 5. Structural data for the first coordination shell obtained from R space fits of $[LnH_n(dota)]^{(n-1)+}$ in solution EXAFS spectra.[a]

	Ln–O(OC)			Ln–O(H_2)			Ln–N		
	N	R [Å]	σ^2 [Å^2]	N	R [Å]	σ^2 [Å^2]	N	R [Å]	σ^2 [Å^2]
$[GdH_n(dota)]^{(n-1)+}$**	3.99	2.39	0.002	5.33	2.44	0.001	–	–	–
$[GdH_n(dota)]^{(n-1)+}$*	3.98	2.40	0.001	2.78	2.41	0.001	1.97	2.65	0.004
$[Gd(dota)]^-$	4.04	2.37	0.007	1.00	2.49	0.001	4.27	2.66	0.009
$[Gd(dota)]^-$[b]	4	2.36	–	1	2.45	–	4	2.66	–
$[EuH_n(dota)]^{(n-1)+}$**	3.98	2.42	0.001	5.38	2.45	0.002	–	–	–
$[Eu(dota)]^+$	3.88	2.38	0.010	1.43	2.51	0.001	4.29	2.66	0.006
$[Eu(dota)]^+$[c]	4	2.39	–	1	2.48	–	4	2.68	–
$[TbH_n(dota)]^{(n-1)+}$**	4.10	2.37	0.003	5.24	2.45	0.010	–	–	–
$[Tb(dota)]^-$	3.87[d]	2.41	0.010	1[d]	2.41	0.010	4.37	2.77	0.010

[a] N = coordination number, R = absorber-neighbor distance, σ = Debye–Waller factor. Estimated uncertainties are ±10% in N, ±0.02 Å in R, and ±0.001 Å^2 in σ^2. [b] From the XRD data of ref. [51]. [c] From XRD data of ref.[52]. [d] Contributions from carboxylic and water oxygen atoms contribution are not discernible. The total coordination number N found by the fitting is equal to 4.87.

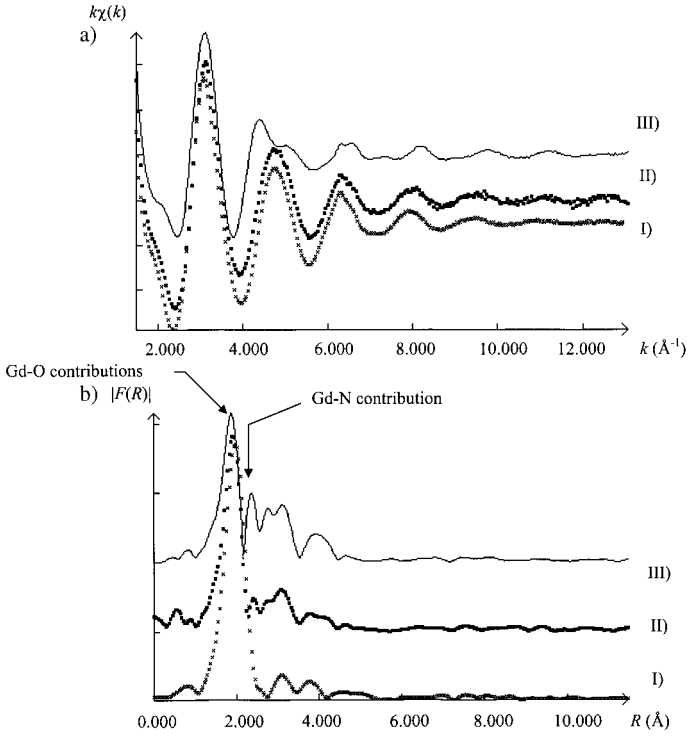

Figure 8. a) Comparison of experimental EXAFS k space spectra and b) the corresponding non-phase-shift-corrected Fourier transforms of Gd–dota complexes at different reaction times between Gd^{3+} and the ligand. I) $t=1$ h, $[GdH_n(dota)]^{(n-1)+}$** complexes; II) $t=100$ h, $[GdH_n(dota)]^{(n-1)+}$* complexes; III) several weeks, $[Gd(dota)]^+$ complexes.

form as a function of time is reported in Figure 8a and 8b, respectively. The $k\chi(k)$ signals show well-defined oscillations up to 12 $Å^{-1}$ (Figure 9a). However, the signal-to-noise ratio is not good owing to the concentration of metal cations in solution. As for the initial compounds, the phase of the oscillations is identical, indicating that the Ln^{3+} ions have similar environments in the three compounds. The complex shapes of the spectra indicates the contribution of various shells of neighbors. Interference is particularly significant at 5.0 $Å^{-1}$ (shoulder), and around 6.3 $Å^{-1}$. The Fourier transforms (Figure 9b) exhibit well-defined features up to about 5.5–6 Å (apparent distances, uncorrected phase shift). As previously shown,[38,52] the first intense peak at around 1.9 Å is related to the carboxylic and water oxygen nearest-neighbors. The exact position of the peak depends on the nature of the central atom. Two other peaks occur at around 2.4 and 3.0 Å, which are attributed to nitrogen and carbon atoms, respectively. A fourth peak is observed near 4 Å, which corresponds to a multiple-scattering contribution, which is confirmed by the multiple-scattering paths obtained by FEFF calculations. The results of the least-squares fittings, reported in Table 5, revealed a mean $Ln–O_{COOH}$ distance close to 2.39 Å, a mean $Ln–O_w$ bond length of 2.47 Å, and an average Ln–N distance close to 2.69 Å. Note that in the case of the Tb^{3+} ion different bond lengths were unexpectedly obtained. Indeed, the $Tb–O_w$ (2.41 Å) and Tb–N (2.77 Å) bonds lengths are, respectively, lower (~2.50 Å) and higher (2.66 Å) than in the Eu^{3+} and Gd^{3+} complexes. The first-shell distances obtained for the $[Eu(dota)]^-$ and $[Gd(dota)]^-$ complexes in solution are similar to those obtained by XRD for the crystals (see Table 5). Consequently, these complexes have the same characteristic distance and geometry in solution as in the solid state. Moreover, our results in solution for the $[Gd(dota)]^-$ compound are in good agreement with EXAFS studies.[52–54]

This EXAFS study confirms unambiguously the existence of intermediate species, and provides reliable information about the lanthanide ion local structure. A first intermediate compound, $[LnH_2(dota)]^+$**, was underlined by the coordination of four carboxylate moieties. The coordination sphere is completed by five water molecules as previously shown with a tetracarboxylated derivative of dota.[38] A second intermediate compound, $[LnH_2(dota)]^+$*, was also characterized in which the metal ion begins to be incorporated into the macrocyclic cavity, and loses two water molecules. Hence, the lanthanide is bonded to four carboxylic oxygen atoms, two macrocyclic cavity nitrogen atoms, and three water molecules. Then, the final complex was obtained in which the four nitrogen atoms are coordinated with only one water molecule still bonded.

Conclusions

The behavior of the three trivalent lanthanide cations (Eu^{3+}, Gd^{3+}, and Tb^{3+}) in the presence of dota is exactly the same. The potentiometric study indicates that the complexation of lanthanide cations to dota involves three phases. The first phase involves the instantaneous formation of complexes as soon as the metal and ligand are mixed, as evidenced by the marked reduction in the pH of the solutions. This is followed by a gradual evolution over 60 h to intermediate complexes that are stable for 80 h. After several weeks, the final thermodynamically stable complexes are formed.

The study by EXAFS of equimolar solutions of dota and Ln^{3+} as soon as the mixture is made shows that Ln^{3+} is bound to four oxygen atoms of the carboxy groups and to five oxygen atoms of water molecules. The nitrogen atoms of the tetraaza ring are not bound to the lanthanide. The presence of five water molecules is confirmed by luminescence in the case of europium and terbium. The schematic representation of the reaction of the first phase of complexation is shown in Scheme 2.

Molecular modeling of the species **1** by Chang et al.[12] in the case of the europium complex $[EuH_2(dota)(OH_2)_5]^+$** by using four Eu–O(OC) bond lengths of 2.35, 2.32, 2.34, and 2.36 Å, and five $Eu–O(H_2)$ bond lengths of 2.59, 2.64, 2.58, 2.55, and 2.62 Å. The two protons of dota are located on two diametrically opposed nitrogen atoms in the tetraaza ring. The Ln^{3+} ion is located above the plane of the oxygen atoms of the carboxylate groups and outside the cage formed by these oxygen atoms and the four nitrogen atoms of the tetraaza ring. An identical configuration was also observed by Jang et al.[33] during the molecular modeling of the $[YH_2(dota)(OH_2)_5]^+$** complex.

The study by EXAFS of the same solutions after a wait time of 60 h shows that the Ln^{3+} ion is still bound to four

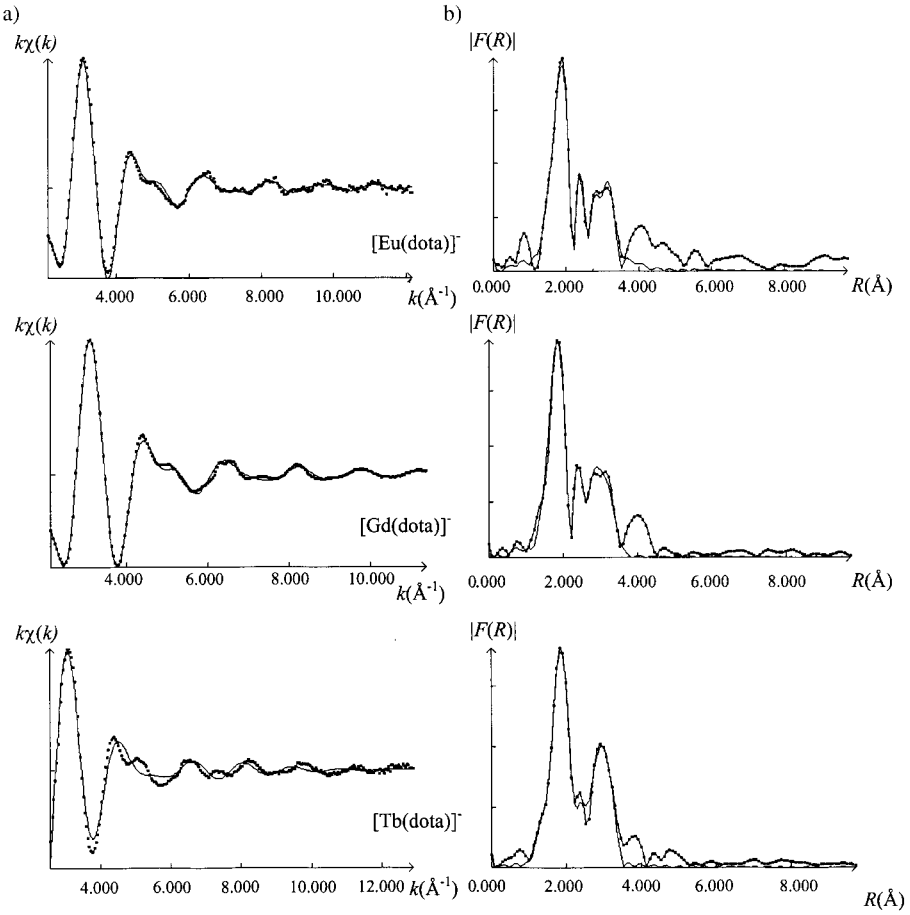

Figure 9. a) k^3-weighted experimental and least-squares fitted EXAFS spectra of the $[Ln(dota)]^-$ final compounds and b) the corresponding non-phase-shift-corrected Fourier transforms. Continuous lines represent the models presented in Table 1.

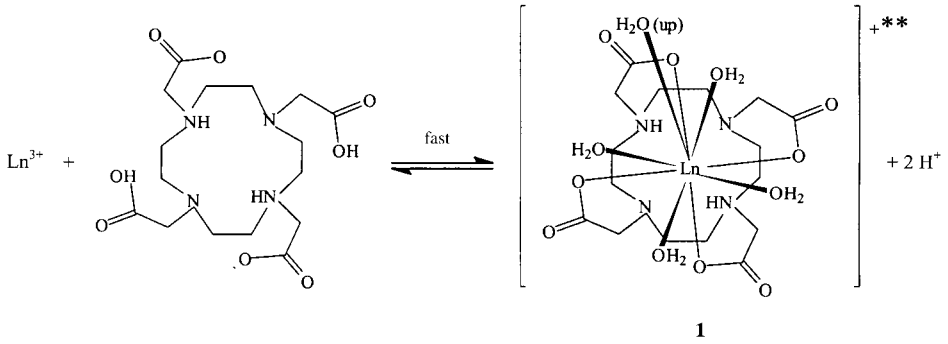

Scheme 2. First complexation step.

oxygen atoms of the carboxy groups, but only three bonds to the oxygen atoms of the water molecules subsist. Two of the nitrogen atoms in the tetraaza ring are now coordinated to the lanthanide. The presence of only three water molecules is confirmed by luminescence in the case of europium and terbium. The potentiometric study shows that the formation of $[LnH_2(dota)]^{+}$* complexes in solution should be envisioned (Figure 2). During the titration of this solution against the base, two protons are neutralized below pH 5. The logarithm of the deprotonation constants is between 2.44 and 2.75 (Table 2), which corresponds more to a deprotonation constant of a carboxylic group than to that of an NH^+ group in the tetraaza ring ($\log K \sim 9$–12). During the molecular modeling of the $[YH_2(dota)(OH_2)_5]^{+}$* complex, Jang et al.[33] noted that the very favorable position of the protons of the two NH^+ groups allows them to migrate from the NH^+ groups to two carboxylate groups. In addition, the calculated transfer energy barrier is low, which also facilitates this migration.

The proposed schematic representation of the reaction for the second phase of complexation corresponds therefore to a concerted rearrangement (Scheme 3): migration of the protons of the two NH^+ groups of compounds **1** and the formation of two Ln^{3+}–N bonds at the expense of two Ln^{3+}–$O(H_2)$ bonds to form the intermediate compounds **2**.

During this phase, the migration of the proton attached to the nitrogen atom and oriented toward the inside of the coordination cage[24,31,33,55] to the oxygen atom of a carboxylate group facilitates its accessibility with respect to OH^- ions. Many authors[13,18,24] have noted that the complexation kinetics are assisted by the OH^- ions. This migration is the only reaction of all the processes that is accelerated by the presence of a base. This mechanism is the inverse of that proposed by Kumar et al.[55] during the dissociation of the $[Gd(dota)]^-$ complex in the presence of a strong acid: protonation of a carboxylate group ($\log K = 2.8$), migration of the proton to a nitrogen atom in the ring and then the rupture of the Gd–N bond.

In fact, the intermediate compounds **2** exist in solution in three forms: $[LnH_2(dota)]^{+}$*, [LnH(dota)]*, and $[Ln(dota)]^{-}$*. The equilibria between these various forms are instantaneous and do not constitute a phase of the complexation mechanism because the most deprotonated form of **2**, $[Ln(dota)]^{-}$*, may also be obtained by direct neutralization of the protons of the NH^+ groups. The formation

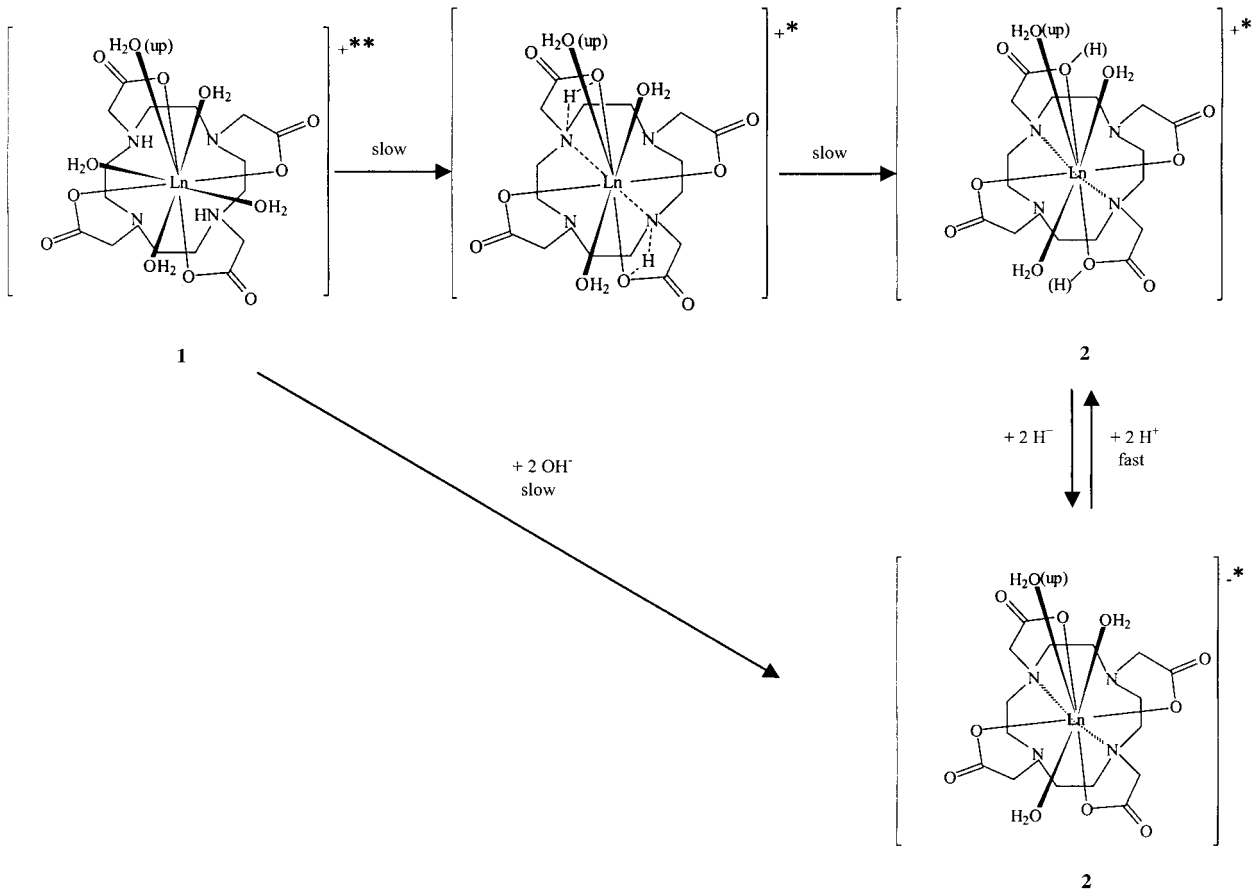

Scheme 3. Second complexation step.

constants of the three complexes ($[LnH_n(dota)]^{(n-1)+*}$, where $n=0$, 1 or 2) were determined by potentiometry in this work (see Table 2). The Gd–N bond lengths measured for the intermediate complexes $[LnH_n(dota)]^{(n-1)+*}$ are similar to those of the final species $[Ln(dota)]^-$ because they are imposed by the size of the macrocyclic cavity.

During the final step, the concerted reorganization of the ligand leading to the formation of two additional Gd–N bonds requires several weeks. The study by EXAFS of the same solutions after 4–6 weeks shows that Ln^{3+} is still bound to the four oxygen atoms of the carboxylate groups, but only one bond to the oxygen atom of a water molecule subsists. The four nitrogen atoms of the tetraaza ring are now coordinated to the lanthanide. The presence of this water molecule is confirmed by luminescence in the case of europium and terbium. The formation constants of the final compounds **3** of formula $[Ln(dota)]^-$ have been calculated ("out-of-cell" method, see Table 3). Molecular modeling of $[Gd(dota)]^-$ and $[Y(dota)]^-$ by Cosentino et al.[56] and Jang et al.,[33] respectively, confirm the lanthanide's position in the "coordination cage" and its environment [four Ln^{3+}–N bonds, four Ln^{3+}–O(OC) bonds, and one Ln^{3+}–$O(H_2)$ bond). The schematic representation of the reaction of this last phase is given in Scheme 4. In this schematic representation, the complexes **2** exist in three forms and are in equilibrium.

The crystalline structures of the complexes $Na[Gd(dota)(H_2O)]$[57,58] and $Na[Eu(dota)(H_2O)]$[51] were determined by X-ray diffraction and have a square-based antiprism geometry. In these compounds, the Ln^{3+} cation is located inside "coordination cage" formed by the four nitrogen atoms of the macro ring and the four oxygen atoms of the carboxy groups; the two planes formed by each type of atom are

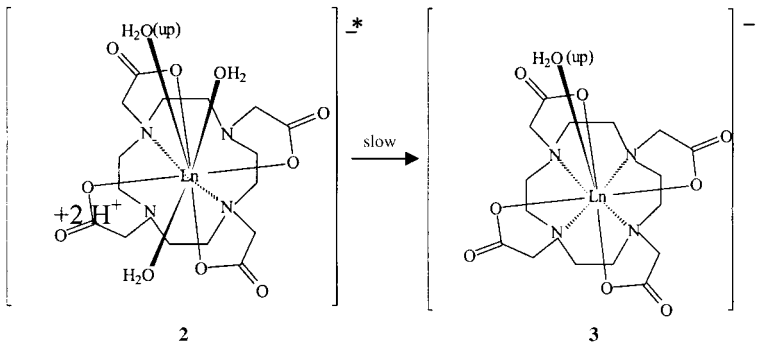

Scheme 4. Third complexation step.

practically parallel. A water molecule caps the plane of the oxygen atoms to assure the coordination number of nine for gadolinium and europium. Bénazeth et al.[52] showed by EXAFS the great similarity of the structures of the $[Gd(dota)]^-$ complex in the solid state and in solution.

In conclusion, three series of successive complexes have been highlighted by at least two methods: the instantaneously formed $[LnH_n(dota)]^{(n-1)+}$** complexes (where $n=0$, 1, and 2) which evolve very rapidly into $[LnH_n(dota)]^{(n-1)+}$* complexes that are stable for 80 h before becoming the final thermodynamically stable $[Ln(dota)]^-$ complexes after several weeks. The coordination mode of the lanthanide, as well as the position of the protons in each of the intermediate and final complexes, have been specified. The migration of the protons of the NH^+ groups of the tetraaza ring to the carboxylate groups has already been proposed during the complexation of the tce-dota ligand.[38] This hypothesis is reinforced for this ligand by the crystallographic study[59] of the $[GdH_5(tce\text{-}dota)]$ complex in which four protons are attached to the four outside carboxylate groups not bound to the Gd^{3+} cation. The fifth proton is effectively attached to an oxygen atom of a carboxylic group bound to gadolinium and not to a nitrogen atom in the ring. The intermediate complexes of europium and terbium with dota had never been studied and the results relating to the final complexes, which are more stable than those of gadolinium, were extremely limited and highly divergent.

Experimental Section

Reagents: All chemicals used were of analytical grade purity. Distilled, argon-bubbled water was used for the preparation of all solutions. The ligand dota was a gift of Guerbet SA. Tetramethylammonium chloride (Fluka Biochemika) was used to control the ionic strength throughout this study. The standard lanthanide (Eu, Gd, Tb) solutions were prepared from the trichloride hexahydrate salts (Aldrich). Their concentrations were determined by edta titrations using xylenol-orange indicator. Carbonate-free solutions of tetramethylammonium hydroxide (Riedel de Haën) were used for potentiometric titrations.

Protometric measurements: The pH-metric measurements used in the determination of protonation and complexation constants were carried out in a thermoregulated cell (25 ± 0.1 °C) with an argon stream flowing over the solution to avoid the dissolution of carbon dioxide. The glass microelectrode Metrohm type T has a low error in the alkaline range. The procedures and apparatus used for protometric measurements have been previously described.[38] The ionic product of water [$pK_w=13.78(1)$ at 25 ± 0.1 °C in 0.1 mol L^{-1} NMe_4Cl] was determined by titration of acetic acid with a CO_2-free NMe_4OH solution.

The protonation constants of dota were determined from nine titrations, which corresponds to 1079 pairs of data; the concentration of the ligand varied from 10^{-3} to 3×10^{-3} mol L^{-1} in the presence of HCl ($0<[HCl]/[dota]<8$).

Study of the intermediate complexes: The intermediate complexes were studied by continuous titration of equimolar mixtures of metal and ligand solutions with NMe_4OH. Since the formation of the intermediate complexes was not instantaneous, it was necessary to determine the speed of base addition. As a result, various titrations of identical equimolar solutions of Ln^{3+} and dota (initial wait time of the mixture one hour; $[Ln^{3+}]=[dota]=1.5\times10^{-3}$ mol L^{-1}; $[NMe_4OH]=0.05$ mol L^{-1}) were performed by varying the stabilization time of the pH after each addition of the base (1–15 min). The titration curves were perfectly superpositioned after 9 minutes of stabilization. In practice, a wait time of 15 minutes was used for each of the three systems.

To study the formation kinetics of the intermediate complexes $[LnH_2(dota)]^+$*, [LnH(dota)]*, and $[Ln(dota)]^-$* (Figure 3), the formation constants of the complexes were calculated from the pairs of data (base volume, pH) obtained by titrating with NMe_4OH (0.05 mol L^{-1}) equimolar solutions of Ln^{3+} and dota ($[Ln^{3+}]=[dota]=2.5\times10^{-3}$ mol L^{-1}) for which the stabilization time of the initial mixture was varied from 1 to 150 h.

Study of the final complexes: The pH evolution of two series of solutions of equimolar mixtures[4] of Gd^{3+} and ligand stored under argon in stoppered flasks in a thermoregulated enclosure was followed at 20 and 50 °C for 10 weeks (1st series: $[dota]=[Gd^{3+}]=10^{-3}$ mol L^{-1}; 2nd series: $[dota]=[edta]=5\times10^{-4}$ mol L^{-1} and $[Gd^{3+}]=10^{-3}$ mol L^{-1}). The complexation kinetics of the Eu–dota and Tb–dota systems were followed at 40 °C in the presence of a strong acid in order to reduce complexation because the complexes formed are more stable than those of gadolinium ($[dota]=[Eu^{3+}$ or $Tb^{3+}]=10^{-3}$ mol L^{-1}, $[HCl]=5\times10^{-3}$ mol L^{-1}).

Under our experimental conditions, the solubility of edta is close to 1.3 mol L^{-1}. The protonation constants of edta were determined from 10 titrations, that is, 1188 pairs of data (base volume, pH); the concentration of edta was varied from 4×10^{-4} to 1.3×10^{-3} mol L^{-1} in the presence of HCl ($4<[HCl]/[dota]<5.2$).

The formation constant of the $[Gd(edta)]^-$ complex was calculated from the 1174 pairs of data (base volume, pH) obtained by continuous titration with NMe_4OH (0.1 mol L^{-1}) of equimolar solutions of Gd^{3+} and edta in the presence of a large excess of HCl ($2.5\times10^{-4}<[edta]=[Gd^{3+}]<5\times10^{-4}$ mol L^{-1} and $10^{-2}<[HCl]<2\times10^{-2}$ mol L^{-1}). The titrations were carried out four hours after mixing the solutions of dota and gadolinium to clear very light complexation kinetics (i.e. the ph of the solutions are stalized after 1 h).

Four series of 40 solutions each were made to determine the formation constant of the intermediate complexes $[Gd(dota)]^-$. The stoppered flasks contained 5 mL of an equimolar mixture of Gd–dota or Gd/(dota and edta) and increasing quantities of NMe_4OH (0.02 mol L^{-1}). They were filled with argon before being closed and then placed in a thermoregulated enclosure for variable stabilization times and at variable temperatures, T. The volumes of added base were selected such that about 30 points were located between pH 2.4 and 4.0, the range over which the intermediate complexes are formed. After the stabilization period, solutions were maintained at 20 °C for a day before the pH values were measured. The concentrations and stabilization temperatures of the various series are as follows: 1st series: $[Gd^{3+}]=[dota]=1.0\times10^{-3}$ mol L^{-1}, $T=50$ °C; 2nd and 3rd series: $[Gd^{3+}]=1.0\times10^{-3}$ mol L^{-1}; $[dota]=[edta]=5.0\times10^{-4}$ mol L^{-1}, $T=50$ and 20 °C); 4th series: $[Gd^{3+}]=[dota]=5.0\times10^{-4}$ mol L^{-1}, $T=20$ °C).

For the Eu–dota and Tb–dota systems, the four series of 40 solutions each have identical concentrations and stabilization temperatures ($[Ln^{3+}]=[dota]=1.0\times10^{-3}$ mol L^{-1}, $[HCl]=5.0\times10^{-3}$ mol L^{-1}, $T=40$ °C).

Protometric computations: The protometric data were processed by using the PROTAF program[60] to obtain the best-fit chemical model and refined overall stability constants β_{mlh}. The program PROTAF,[60] which is based on the weighted least-squares of the residues of the experimental variables (volume of titrant, pH), allows simultaneous processing of 10 titrations, each including 150 pairs of data (volume, pH).

Luminescence measurements: The measurements were determined in D_2O/H_2O mixtures, the molar fraction of H_2O varying from a value close to 0 to a value of 1. To measure the luminescence of the initial complexes, solutions of lanthanide chloride (10^{-3} mol L^{-1}) and dota (5×10^{-3} mol L^{-1}) were prepared that contained a high ligand/metal ratio to avoid the formation of the nonahydrated lanthanide ion. For the intermediate complexes, a concentrated equimolar solution of dota and $EuCl_3$ (5×10^{-2} mol L^{-1}) was prepared in H_2O. After 50 h, this solution was then diluted to 1/10 in H_2O and D_2O just before the measurements were taken. For the final complexes, equimolar solutions of dota and lanthanide chloride (2.5×10^{-2} mol L^{-1}) were prepared at a pH near 6.9, and were kept for 2 weeks at 40 °C before measurements were taken.

Luminescence spectra for europium and terbium were recorded on a Perkin-Elmer LS50B spectrometer equipped with a Hamamatsu R928

[4] The total quantity of ligand was always slightly greater than that of Ln^{3+} to prevent any possible precipitation of the hydroxide $Ln(OH)_3$.

photo-multiplier and operating in a time-resolved mode. Lifetimes were measured at 25 °C by excitation of the sample solution by a short pulse of light (europium species: 394 nm; terbium species: Tb^{3+} 221 nm, Tb-P730 229 nm). The emission was monitored at 616 nm for Eu^{III} and at 544 nm for Tb^{III} by using the Lemming Ver 1.01 program. The gate time was 0.1 ms and the slit widths were 15 and 5 nm for Eu^{III} and 10 and 5 nm for Tb^{III}. The rate constants, k, and the inverse of the lifetimes, τ, are the average values of 10 series of 20–40 measurements for each D_2O/H_2O mixture. The luminescence decay curves were fitted by Equation (11) by using the general curve fitting program Origin. High correlation coefficients were determined. The quoted k_{D_2O} values were estimated and the k_{H_2O} values verified from linear extrapolation of k versus the molar fraction of H_2O.

$$F = F_o \exp^{(-kt)} \tag{11}$$

EXAFS study: **X-ray absorption data collection and processing**: The EXAFS (extended X-ray absorption fine structure) data were collected at LURE (Laboratoire d'Utilisation du Rayonnement Electromagnétique, Paris-Sud University) on the XAS 4 beam line of the DCI storage ring (positron energy = 1.85 GeV; mean current = 300 mA). The spectra were recorded at the lanthanide L_3 edge using a Si(111) channel-cut monochromator, which was detuned to 30% of the maximal intensity for Eu and Gd and 15% for Tb to remove the higher-order harmonics. The measurements were performed at room temperature in the transmission mode with two low pressure ($\approx$0.2 atm) air-filled ionisation chambers.

Each spectrum is the sum of three to four recordings in the range of 150 eV below to 600–700 eV above the absorption edge, since the range of the L_3 edge (E_{L3} = 6977 eV, 7243 eV, and 7515 eV for Eu, Gd, and Tb, respectively) XAFS is limited by the presence of the Ln^{III} L_2 edge (E_{L2} = 7618 eV, 7931 eV, and 8252 eV for Eu, Gd, and Tb, respectively). Spectra were recorded using sampling steps of 2 eV with an integration time of 2.0 s per point.

The EXAFS spectra at the Ln^{III} L_3 edge were measured in aqueous solution at room temperature. The solutions were obtained by the reaction of dota (0.11 mol L^{-1}) with the appropriate lanthanide (0.1 mol L^{-1}) in deionized water. Then the pH was adjusted to 6.9 for the final compounds, and to around 2.1 for the intermediate ones. The samples were then added to cells whose thickness varied between 1 and 3 mm. In all cases, we optimized the experimental parameters in order to obtain a jump to the X-ray absorption edge of between 0.5 and 1.

Data analysis was performed by means of the "EXAFS pour le Mac" package.[61] The $\chi(k)$ functions were extracted from the data[62–64] with a linear pre-edge background, a combination of polynomials, and spline atomic-absorption background, and normalized by using the Lengeler–Eisenberg method.[65] The energy threshold, E_0, was measured at the middle of the absorption edge and was corrected for each spectrum in the fitting procedure. The k^3 weighted $\chi(k)$ function was Fourier transformed in the range of k = 2–13 Å^{-1} by means of a Kaiser–Bessel window with a smoothness parameter τ equal to 2.5 (k is the photoelectron wave number). In this work, all Fourier transforms were calculated and presented without phase correction. The peaks corresponding to the first or two first coordination shells were then isolated and back-Fourier transformed into k space to determine the mean coordination number, N, the bond length, R, and the Debye–Waller factor, σ, by a fitting procedure realized in the framework of single scattering using the standard EXAFS formula (12).The backscattering phase, $\Phi_i(k,R_i)$, and amplitude, $A_i(k,R_i)$,

$$\chi(k) = S_0^2 \sum_i \left\{ \frac{N_i}{R_i^2} Ai(k) e^{-2\sigma_i^2 k^2} e^{-2R_i/\lambda(k)} \sin\left[2kR_i + \Phi_i(k)\right] \right\} \tag{12}$$

functions were obtained by using experimental and theoretical approaches. The experimental backscattering phase, $\Phi_i(k,R_i)$, and amplitude, $A_i(k,R_i)$, functions were extracted from the EXAFS data of model compounds of known crystallographic structure: aqueous rare earth solution,[53] $[Gd(dota)(H_2O)]^-$,[52] $[Eu(dota)(H_2O)]^-$,[51] and $[Tb(teta)(H_2O)]^-$,[66]. The theoretical backscattering functions were calculated by using the ab initio FEFF7 program,[67] with input data based on the X-ray crystal structure. Moreover, the FEFF7 program[53] was used to check if the multiple scattering of our reference compounds of known crystallographic structure is negligible in the 0–3.4 Å range (see text).

[1] R. B. Laufer, *Chem. Rev.* **1987**, *87*, 901–927.
[2] M. F. Tweedle in *Lanthanide Probes in Life*, Chemical and Earth Sciences (Eds.: J. C. Bünzli, G. G. Choppin), Amsterdam, Elsevier, **1989**, p. 127.
[3] H. Gries in *Contrast Agent (I) Magnetic Resonance Imaging*, Topics in Current Chemistry (Ed.: W. Krause), Berlin, Heidelberg, Springer, **2002**.
[4] K. Kumar, M. F. Tweedle, *Pure Appl. Chem.* **1993**, *65*, 515.
[5] S. Aime, M. Botta, M. Fasano, E. Terreno, *Chem. Soc. Rev.* **1998**, *27*, 19–29.
[6] P. Caravan, J. J. Ellison, T. J. McMurry, R. B. Lauffer, *Chem. Rev.* **1999**, *99*, 2293–2352.
[7] A. Bianchi, L. Calabi, C. Giorgi, P. Losi, P. Mariani, P. Paoli, P. Rossi, B. Valtancoli, M. Virtuani, *J. Chem. Soc. Dalton Trans.*, **2000**, 697–705.
[8] J. M. Lehn, J. P. Sauvage, *J. Am. Chem. Soc.* **1975**, *97*, 6700–6707.
[9] J. Dale, *Isr. J. Chem.* **1980**, *20*, 3.
[10] S. P. Artz, D. J. Cram, *J. Am. Chem. Soc.* **1984**, *106*, 2160–2171.
[11] R. D. Hancock, A. E. Martell, *Chem. Rev.* **1989**, *89*, 1875–1914.
[12] C. A. Chang, Y. L. Liu, C. Y. Chen, X. M. Chou, *Inorg. Chem.* **2001**, *40*, 3448–3455.
[13] K. Kumar, M. F. Tweedle, *Inorg. Chem.* **1993**, *32*, 4193–4199.
[14] J. F. Desreux, *Inorg. Chem.* **1980**, *19*, 1319–1324.
[15] S. Aime, M. Botta, G. Ermondi, *Inorg. Chem.* **1992**, *31*, 4291–4299.
[16] S. Hoeft, K. Roth, *Chem. Ber.* **1993**, *126*, 869–873.
[17] S. Aime, M. Botta, M. Fasano, M. P. Marques, C. F. Geraldes, D. Pubanz, A. E. Merbach, *Inorg. Chem.* **1997**, *36*, 2059–2068.
[18] E. Brücher, G. Laurenczy, Z. S. Makra, *Inorg. Chim. Acta* **1987**, *139*, 141–142.
[19] E. Brücher, A. D. Sherry, *Inorg. Chem.* **1990**, *29*, 1555–1559.
[20] S. P. Kasprzyk, R. G. Wilkins, *Inorg. Chem.* **1982**, *21*, 3349–3352.
[21] X. W. Wang, T. Jin, V. Comblin, A. Lopez-Mut, E. Merciny, J. F. Desreux, *Inorg. Chem.* **1992**, *31*, 1095–1099.
[22] E. Szilagyi, E. Toth, Z. Kovacs, J. Platzek, B. Raduchel, E. Brücher, *Inorg. Chim. Acta* **2000**, *298*, 226–234.
[23] A. Bianchi, L. Calabi, L. Ferrini, P. Losi, F. Uggeri, B. Valtancoli, *Inorg. Chim. Acta* **1996**, *249*, 13–15.
[24] E. Toth, E. Brücher, I. Lazar, I. Toth, *Inorg. Chem.* **1994**, *33*, 4070–4076.
[25] E. T. Clarke, A. E. Martell, *Inorg. Chim. Acta* **1991**, *190*, 37–46.
[26] V. Comblin, D. Gilsoul, M. Hermann, V. Humblet, V. Jacques, M. Mesbahi, C. Sauvage, J. F. Desreux, *Coord. Chem. Rev.* **1999**, *185–186*, 451–470.
[27] S. L. Wu, W. De W. Horrocks, Jr., *J. Chem. Soc. Dalton Trans.* **1997**, 1497–1502
[28] W. P. Cacheris, S. K. Nickle, A. D. Sherry, *Inorg. Chem.* **1987**, *26*, 958–960.
[29] M. F. Loncin, J. F. Desreux, E. Mercini, *Inorg. Chem.* **1986**, *25*, 2646–2648.
[30] E. Toth, R. Kiraly, J. Platzec, E. Brücher, *Inorg. Chim. Acta* **1996**, *249*, 191–199.
[31] S. L. Wu, W. De W. Horrocks, Jr., *Inorg. Chem.* **1995**, *34*, 3724–3732.
[32] L. Burai, I. Fabian, R. Kiraly, E. Szilagyi, E. Brücher, *J. Chem. Soc. Dalton Trans.* **1998**, 243–248.
[33] Y. H. Jang, M. Blanco, S. Dasgupta, D. A. Keire, J. E. Shively, W. A. Goddard III, *J. Am. Chem. Soc.* **1999**, *121*, 6142–6151.
[34] K. Kumar, T. Jin, X. Wang, J. F. Desreux, M. F. Tweedle, *Inorg. Chem.* **1994**, *33*, 3823–3829.
[35] J. F. Desreux, E. Merciny, M. F. Loncin, *Inorg. Chem.* **1981**, *20*, 987–991.
[36] E. T. Clarke, A. E. Martell, *Inorg. Chim. Acta* **1991**, *190*, 28–36.
[37] R. Delgado, Y. Sun, J. Motekaitis, A. E. Martell, *Inorg. Chem.* **1993**, *32*, 3320–3326.
[38] J. Moreau, E. Guillon, P. Aplincourt, J. C. Pierrard, J. Rimbault, M. Port, M. Aplincourt, *Eur. J. Inorg. Chem.* **2003**, 3007–3020.
[39] E. Toth, E. Brücher, *Inorg. Chim. Acta* **1994**, *221*, 165–167.
[40] K. Kumar, C. A. Chang, L. C. Francesconi, D. D. Dischino, M. F. Malley, J. Z. Gougoutas, M. F. Tweedle, *Inorg. Chem.* **1994**, *33*, 3567–3575.

[41] H. Stetter, W. Frank, *Angew. Chem.* **1976**, *88*, 722; *Angew. Chem. Int. Ed.* **1976**, *15*, 686.
[42] R. Delgado, F. J. J. R. Da Silva, *Talanta* **1982**, *25*, 815–822.
[43] C. G. Pippin, T. J. McMurry, M. W. Brechbiel, M. McDonald, R. Lambrecht, D. Milenic, M. Rosseli, D. Colcher, O. A. Ganswow, *Inorg. Chim. Acta* **1995**, *239*, 43–51.
[44] S. Aime, P. L. Anelli, M. Botta, F. Fideli, M. Grandi, P. Paoli, F. Uggeri, *Inorg. Chem.* **1992**, *31*, 2422–2428.
[45] S. Chaves, R. Delgado, F. J. J. R. Da Silva, *Talanta* **1992**, *35*, 249–254.
[46] A. Bianchi, L. Calabi, F. Corana, S. Fontana, P. Losi, A. Maiocchi, L. Paleari, B. Valtancoli, *Coord. Chem. Rev.* **2000**, *204*, 309–393.
[47] M. F. Tweedle, J. J. Hagan, K. Kumar, S. Mantha, C. A. Chang, *Magn. Reson. Imaging* **1991**, *9*, 409–415.
[48] J. F. Desreux, *Bull. Univ. Md. Sch. Med.* **1979**, *64*, 814–839.
[49] R.M. Supkowski, W. De W. Horrocks, Jr., *Inorg. Chim. Acta* **2002**, *340*, 44–48
[50] W. De W. Horrocks, Jr., D. R. Sudnick, *J. Am. Chem. Soc.* **1979**, *101*, 334–340.
[51] M. R. Spirlet, J. Rebizant, J. F. Desreux, M. F. Loncin, *Inorg. Chem.* **1984**, *23*, 359–363.
[52] S. Benazeth, J. Purans, M. C. Chalbot, M. K. Nguyen-Van-Duong, L. Nicolas, F. Keller, A. Gaudemer, *Inorg. Chem.* **1998**, *37*, 3667–3674.
[53] T. Yamaguchi, M. Nomura, H. Wakita, H. Ohtaki, *J. Chem. Phys.* **1988**, *89*, 5153–5159.
[54] J. A. Solera, J. Garcia, M. G. Proietti, *Phys. Rev. B* **1995**, *51*, 2678–2686.
[55] K. Kumar, C. A. Chang, M. F. Tweedle, *Inorg. Chem.* **1993**, *32*, 587–593.
[56] U. Cosentino, A. Villa, D. Pitea, G. Moro, V. Barone, A. Maiocchi, *J. Am. Chem. Soc.* **2002**, *124*, 4901–4909.
[57] J. P. Dubost, J. M. Leger, M. H. Langlois, D. Meyer, M. Schaffer, *C. R. Acad. Sci. Ser. II* **1991**, *312*, 349–354.
[58] C. A. Chang, L. C. Francesconi, M. F. Malley, K. Kumar, J. Z. Gougoutas, M. F. Tweedle, D. W. Lee, L. J. Wilson, *Inorg. Chem.* **1993**, *32*, 3501–3508.
[59] M. Woods, S. Aime, M. Botta, J. A. K. Howard, J. M. Moloney, M. Navet, D. Parker, M. Port, O. Rousseaux, *J. Am. Chem. Soc.* **2000**, *122*, 9781–9792.
[60] R. Fournaise, C. Petitfaux, *Talanta* **1987**, *30*, 385–395.
[61] A. Michalowicz, *Logiciel pour la chimie*, Société Française de Chimie, *Paris* **1991**, 102.
[62] B. K. Teo, *Inorganic Chemistry Concepts, EXAFS: Basic Principles and Data Analysis*, Springer, Berlin, **1986**, p. 9.
[63] D. C. Köningsberger, R. Prins, *X-ray Absorption Principles, Applications, Techniques of EXAFS, SEXAFS and XANES*, Wiley, New York, **1988**.
[64] F. W. Lytle, D. E. Sayers, E. A. Stern, *Co-Chairmen Report of the International Workshop on Standards and Criteria in X-ray Absorption Spectroscopy, Physica* **1989**, *B158*, 701.
[65] B. Lengeler, P. Eisenberger, *Phys. Rev. B* **1980**, *21*, 4507–4520.
[66] M. R. Spirlet, J. Rebizant, M. F. Loncin, J. F. Desreux, *Inorg. Chem.* **1984**, *23*, 4278–4283.
[67] S. I. Zabinsky, J. J. Rehr, A. Ankudinov, R. C. Albers, M. J. Eller, *Phys. Rev. B* **1995**, *52*, 2995–3009.

Received: January 5, 2004
Published online: September 13, 2004

